Food Chemistry 368 (2022) 130775

Contents lists available at ScienceDirect

Food Chemistry

journal homepage: www.elsevier.com/locate/foodchem

Profiling the annual change of the neurobiological and antioxidant effects of five *Origanum* species in correlation with their phytochemical composition

Hasya Nazli Gök [a,1], Simon Vlad Luca [b,c,1], Saadet Tugrul Ay [d], Łukasz Komsta [e], Ramin Ekhteiari Salmas [f], Ilkay Erdogan Orhan [a,*], Krystyna Skalicka-Woźniak [g,*]

[a] Department of Pharmacognosy, Faculty of Pharmacy, Gazi University, 06330 Ankara, Turkey
[b] Biothermodynamics, TUM School of Life Sciences, Technical University of Munich, 85354 Freising, Germany
[c] Department of Pharmacognosy, "Grigore T. Popa" University of Medicine and Pharmacy Iasi, 700115 Iasi, Romania
[d] Antalya Metropolitan Municipality, Department of Agricultural Services, 07310 Antalya, Turkey
[e] Department of Medicinal Chemistry, Medical University of Lublin, 20-093 Lublin, Poland
[f] Department of Chemistry, Britannia House, King's College London, SE1 1DB, United Kingdom
[g] Independent Laboratory of Natural Products Chemistry, 1 Chodzki Str, Medical University of Lublin, 20-093 Lublin, Poland

ARTICLE INFO

Keywords:
Origanum
Oregano
Cholinesterase
Antioxidant
HPLC-DAD-ESI/HRMS
Correlation

ABSTRACT

The ethanol extracts of five *Origanum* species: *O. majorana* L., *O. onites* L., *O. syriacum* L., *O. vulgare* subsp. *hirtum* (Link) Ietsw., and *O. vulgare* subsp. *viride* (Boiss.) Hayek, collected annually (each month), were investigated for their cholinesterase inhibition and antioxidant effects. The phytochemical composition of a total of 60 extracts was assessed by HPLC-DAD-ESI/HRMS, revealing the presence of a total of 73 compounds. Possible correlation between the bioactivity and metabolite profiles during 12 months was monitored. Acetylcholinesterase (AChE) inhibitory activity was found to be the highest between April and November (50.29–75.95%, 200 μg/mL), while the highest inhibition towards butyrylcholinesterase (BChE) was observed for the extracts between April and October (71.68–88.97%). Aromadendrin showed good correlation with anti-AChE, anti-BChE and reducing power activities. Furthermore, molecular docking data with aromadendrin, caffeoylarbutin and eriodictyol indicated that caffeoylarbutin had the lowest binding energy against both enzymes.

1. Introduction

Origanum L., represented by 43 species in the world and 21 species in Turkey, belongs to Lamiaceae family (Özer et al., 2020). Various species of *Origanum* are used against many disorders in Anatolian folk medicine as well as food spices and herbal teas. Among them, *O. vulgare* L. C. Koch is used as diuretic or to treat intestinal pain, colds and stomachache; *O. vulgare* L. subsp. *viride* (Boiss.) Hayek for dyspepsia and stomachache; *O. vulgare* L. subsp. *vulgare* for wound healing; *O. majorana* L. against colds and catarrh; *O. dubium* Boiss. against colds and stomachache; *O. minutiflorum* O. Schwarz & P.H. Davis against stomachache, toothache, and rheumatism; *O. onites* L. against colds, stomachache, stiff shoulder, abdominal pain, rheumatism, back pain, and stomach disorders (Honda et al., 1996; Yeşilada et al., 1995). Previous phytochemical studies of *Origanum* species indicated a rich chemical content, including monocyclic monoterpenes, bicyclic monoterpenes, sesquiterpenes, diterpenoids, triterpenoids, phenolic acids, and flavonoids (Marrelli, Statti, & Conforti, 2018). The relevant *in vitro* and *in vivo* studies demonstrated that many *Origanum* species possess antidiabetic, anti-obesity, antihyperlipidemic, hepatoprotective, anti-urolithic, antimicrobial, antioxidant, antiproliferative, antinociceptive, antiplatelet, anti-melanogenic, anxiolytic, anti-inflammatory, memory enhancer and cytotoxic activities (Marrelli et al., 2018; Naquvi, Ahamad, Salma, Ansari, & Najmi, 2019).

Alzheimer's disease (AD) is a neurodegenerative and progressive disorder that generally occurs in elderly population. It is estimated that the number of people suffering from dementia would reach approximately 106.2 million by 2050 (Brookmeyer, Johnson, Ziegler-Graham,

* Corresponding authors.
E-mail addresses: iorhan@gazi.edu.tr (I.E. Orhan), kskalicka@pharmacognosy.org (K. Skalicka-Woźniak).
[1] Both authors share co-first authorship.

https://doi.org/10.1016/j.foodchem.2021.130775
Received 18 March 2021; Received in revised form 2 August 2021; Accepted 2 August 2021
Available online 5 August 2021
0308-8146/© 2021 Elsevier Ltd. All rights reserved.

& Arrighi, 2007). Several mechanisms that can play a role in the pathophysiology of AD are scrutinized under "amyloid hypothesis" and "cholinergic hypothesis". Accordingly, AD can be caused by the formation of neuritic plaques and neurofibrillary tangles (NFTs), chronic neuroinflammation, neuronal injury and synapse loss . Relevantly, the inhibition of the enzyme family called cholinesterases (ChEs), consisting of two sister enzymes, *i.e.* acetylcholinesterase (AChE) and butyrylcholinesterase (BChE), is critical; the ChE inhibitors are at the moment the most often prescribed drugs for the treatment of AD (Weller & Budson, 2018). AChE induces the hydrolysis of the neurotransmitter acetylcholine (ACh) which occurs in insufficient levels in the brain of AD patients. Hence, AChE inhibitors provide the balanced levels of ACh. On the other hand, BChE has been found to occur in excessive amounts in amyloid plaques in AD patients and thus, the inhibition of BChE is also important, especially in the latest stage of the disease (Darvesh et al., 2012). Increased oxidative stress is associated with neuronal DNA damage in AD. Oxidative stress may cause mitochondrial dysfunction and decreased mitophagy and sirtuin activity. The main sources of the oxidative stress in AD are the metal ions, in particular copper, iron and zinc. It was suggested that the transition metal homeostasis in the brain and cerebrospinal fluid of AD patients is imbalanced (Moreira et al., 2008). Reactive oxygen species (ROS) are also connected with the pathogenesis of neurodegenerative diseases including AD. The studies demonstrated that hydroxyl radicals, hydrogen peroxide, nitric oxide and superoxide anions play key roles in the oxidative stress-mediated neurodegeneration in AD, causing mitochondrial dysfunction. In this regard, the inhibition of both AChE and BChE as well as a strong antioxidant activity seem to be very important for any novel drug candidate towards AD.

Biosynthetic processes consistently continue in plants throughout the year. As the presence and concentration of chemical substances change, their biological effects can thereby be affected. Consequently, the current study focused on assessing cholinesterase inhibitory and antioxidant effects in connection with the phytochemical profile of *O. majorana* L., *O. onites* L., *O. syriacum* L., *O. vulgare* subsp. *hirtum* (Link) Ietsw., and *O. vulgare* subsp. *viride* (Boiss.) Hayek collected in a 12 month-duration period throughout a year.

2. Material and methods

2.1. Plant materials

The parent plant materials were collected from Antalya-Alanya town /Mahmutlar vicinity- altitude of 778 m (*O. majorana* L.), Antalya - Kemer-Olimpos National Park – altitude of 34 m (*O. onites* L.), Antalya - Gebiz-Haskızılören-Bozburun Mountain - altitude of 678 m (*O. syriacum* L.), Antalya-Etler town/Ovacık district - altitude of 900 m (*O. vulgare* subsp. *hirtum* (Link) Ietsw.), and Antalya- Alanya town, Kozlu River vicinity - altitude of 993 m (*O. vulgare* L.) in 2002. The collected species were recultivated later and collected neatly from January to December in 2014.

2.2. Extraction

The aerial parts of the *Origanum* species were dried at the room temperature and ground to the homogeneous fine powder in a mechanical grounder. The powdered plant materials were macerated in ethanol (80%) for 3 days. The ethanolic parts were filtered, and evaporated under vacuum at the 45 °C until dryness. The crude extracts obtained were kept at 4 °C prior to the activity and phytochemical experiments. The yields (%, w/w) of the crude extracts were given in Table S1 (Appendix A).

2.3. Cholinesterase inhibitory activity assays

The AChE and BChE enzyme inhibitory activities of the extracts were determined using the Ellman's method (Ellman, Courtney, Andres, & Featherstone, 1961) with a slight modification utilizing microtiter assay (VersaMax Molecular Devices, USA). The extracts (20 μL) were incubated with electric eel AChE (Sigma, Type-VI-S, EC 3.1.1.7) and horse serum BChE (EC 3.1.1.8, Sigma) used as the enzyme sources (20 μL) in phosphate buffer (pH 8, 140 μL) for 10 min in 25 °C. After the incubation, acetylthiocholine iodide and butyrylthiocholine chloride were added as the substrates (10 μL) for AChE and BChE inhibitory activity, respectively. Simultaneously, 5,5-dithio-bis(2-nitrobenzoic) acid (DTNB, Sigma, St. Louis,MO, USA) (10 μL) was added as the coloring reagent. The formation of the yellow 5-thio-2-nitrobenzoateanion with thiocholines was measured at a wavelength of 412 nm. Galanthamine was used as the reference drug. Analyses were performed in triplicate. The AChE/BChE inhibitory activities were calculated by using the formula given below:

$$\text{Enzyme inhibitory activity}(\%) = 1 - \frac{Reaction\ rate\ of\ sample\ at\ 412\ nm}{Reaction\ rate\ of\ control\ at\ 412\ nm} x100$$

2.4. Antioxidant activity assays

2.4.1. DPPH radical scavenging assay

The 2,2-diphenyl-1-picrylhydrazyl (DPPH) radical scavenging activity of the extracts was determined by a slight modification of the method of Hatano, Kagawa, Yasuhara, and Okuda (1988). DPPH solution was mixed with extracts then incubated for 30 min in darkness. The absorbance of the mixtures was read at 514 nm. Quercetin was used as the reference. Analyses were run in triplicate. The percentage of DPPH inhibition was calculated as given below:

$$\%\text{inhibition} = \frac{Absorbance\ of\ control\ -\ Absorbance\ of\ test\ sample}{Absorbance\ of\ control} x100$$

2.4.2. Metal-chelation capacity assay

The metal-chelation capacity of the extracts was determined by a slight modification of the method of Chua, Tung, and Chang (2008) by Fe^{+2}-ferrozine test system using ELISA microplate reader. Firstly, 2 mM $FeCl_2$ solution was added to the extract dilutions, then the reaction started with the addition of the 40 μL of ferrozine solution. After the 10 min of the reaction, the absorbance of the mixtures was read at 562 nm. Ethylenediamine tetraacetic acid (EDTA) was used as the reference. Analyses were run in triplicate. The inhibition of ferrozine-Fe^{2+}complex formation was measured by using the formula given below:

$$\%\text{inhibition} = \frac{Absorbance\ of\ control\ -\ Absorbance\ of\ test\ sample}{Absorbance\ of\ control} x100$$

2.4.3. Ferric-reducing antioxidant power (FRAP) assay

FRAP activity of the extracts was determined by a slight modification of the method of Oyaizu (1986). The extracts were incubated with potassium ferricyanide in phosphate buffer (pH 6.6) for 20 min at 50 °C. Then, $FeCl_3$ (0.1%, w/v) and distilled water were added. After 30 min of the reaction, the absorbance of the mixtures was read at 700 nm by ELISA microplate reader. Quercetin was used as the reference. Analyses were run in triplicate. In this assay, higher absorbance of the reaction indicates higher reducing power.

2.5. HPLC-DAD-ESI/HRMS analysis

The high-performance-diode array detector-electrospray ionization/high-resolution mass spectrometry (HPLC-DAD-ESI/HRMS) analyses of the *Origanum* extracts were performed using the procedures described by Luca et al. (2019) with several modifications. An Agilent 1200 Series HPLC system (Agilent Technologies, Palo Alto, CA, USA) equipped with a binary pump (1312C), column thermostat (1316A), auto-sampler (1329B), DAD (1315D) and a high-resolution accurate-mass quadrupole-time-of-flight mass spectrometer (HR-AM-QTOF-MS 6530B)

was used. The separations were carried out on an Phenomenex Gemini RP-18 (100 mm × 2 mm; i.d. 3 μm) column with a mobile phase composed of 0.1% formic acid in water (solvent A) and 0.1% formic acid in acetonitrile (solvent B) and the following linear gradient: 0–40 min 5–60% B; 41–50 min 95% B; post-time 20 min. The flow rate was 0.4 ml/min, while the sample injection volume was 10 μL. The UV spectra were recorded over the wavelength domain of 190–400 nm. The subsequent MS operating parameters were applied: ESI negative ion mode; mass-to-charge (*m/z*) range 100–1500; drying gas (nitrogen) temperature 300 °C; drying gas flow 12 L/min; sheath gas temperature 325 °C; sheath gas flow 12 L/min; nebulizer pressure 40 psi; capillary voltage 4000 V; nozzle voltage 2000 V; fragmentor voltage 140 V; skimmer voltage 65 V; radiofrequency voltage 750 V; collision induced dissociation voltages 15 and 40 V. Data analysis was processed with Mass Hunter Qualitative Analysis B.08.00 (Agilent Technologies) software. The assignment of the peaks observed in the base peak chromatograms (BPC) of the six *Origanum* samples was carried out by comparing the spectrometric data with previous literature data reporting on the LC-MS analysis of similar constituents (Table 4) or online databases (METLIN, KNApSacK, PubChem, NIST Chemistry WebBook).

2.6. Statistical analysis

Statistical analysis of the enzyme inhibition and antioxidant activity results was evaluated by ANOVA (one way) and Dunnett's multiple comparison test. $p < 0.05$ was considered to be significant ($^{*}p < 0.05$; $^{**}p < 0.01$; $^{***}p < 0.001$). The statistical analysis of correlations was done with Pearson's test for significance of correlation coefficient. All computations were done in GNU R 4.0 under R Studio 1.4 environment.

2.7. Ligand-binding energy calculation

Crystal structures of AChE and BChE with the IDs of 4EY7 (Cheung, 2012) and 5DYW (Kosak, 2016) were retrieved from the Protein Data Bank (PDB) (). The structures were prepared for docking simulations using the Protein Preparation Wizard tool of Schrödinger software (Madhavi Sastry, Adzhigirey, Day, Annabhimoju, & Sherman, 2013). The preparation process consists of adding missing atoms and hydrogen atoms, assigning bond orders, creating disulfide bonds, deleting water molecules beyond 5 A from HET groups, biological pH assigning using the PROPKA tool () and applying restrained minimization using the OPLS3 force field. The structures of the ligands downloaded from PubChem were minimized to their lowest energies and ionized at a biological pH. Ligand binding energies of the selected compounds, including Aromadendrin, Caffeoylarbutin and Eriodictyol were estimated using Induced Fit Docking (IFD) method implemented in Schrödinger software (Farid, Day, Friesner, & Pearlstein, 2006). Galanthamine is also used as a reference compound to be compared with the other compounds. IFD is a feasible docking method to apply a ligand- and receptor flexible simulation to generate more possible docking poses inside the active site and then their binding energies are calculated separately. The coordinates of the co-crystal ligands were used to determine the ligand-binding domains of the both targets.

3. Results and discussion

3.1. Enzyme inhibitory and antioxidant activities

While *O. majorana* displayed the AChE inhibitory activity above 50% during the 9 months of the year, *O. onites* did not exert remarkable inhibitory activity during all year. The lowest IC_{50} value of *O. majorana* was in August (62.08 μg/ml). *O. syriacum* generally exerted higher activity on AChE in the spring months (April, May, and June) and in autumn (October and November). The highest AChE inhibition of *O. vulgare* was observed in April ($IC_{50} = 125.30$ μg/ml). *O. vulgare* subsp. *hirtum* inhibited the AChE between May and December in different percentages (Table 1, Fig. 1). BChE enzyme inhibitory results demonstrated that all taxa displayed notable activity. The lowest IC_{50} value was shown in the *O. syriacum* October extract (40.19 μg/ml) (Table 2).

Considering the antioxidant activity findings, most of the extracts displayed marked DPPH radical scavenging activity over 50% (Table S2). This activity for the extracts tested was observed to be different from each other, which did not give a definite correlation at monthly level. The strongest DPPH radical scavenging activity was found in *O. syriacum* from January and February collections. Metal ions, such as Cu (II) and Fe (III), form the oxidative stress in the brain, therefore in the AD therapy metal chelators and antioxidants play a remarkable role (Budimir, 2011). However, most of the *Origanum* extracts displayed no or low metal-chelation activity. Only *O. vulgare* subsp. *hirtum* extract of September collection displayed metal-chelation activity above 50% at 2000 μg/ml concentration. Although many extracts showed high FRAP activity, the extracts of *O. syriacum* from January ($A_{700nm} = 1.37$) and February ($A_{700nm} = 1.57$) exhibited the highest FRAP activity at 2000 μg/ml (Table 3).

3.2. HPLC-DAD-ESI/HRMS metabolite profiling of the Origanum extracts

The HPLC-DAD-ESI/HRMS analysis of the 60 extracts prepared from five *Origanum* species led to annotating a total number of 73 peaks, including 21 flavonoids, 13 fatty acid derivatives, nine phenolic acids, five diterpenes, four monoterpenes glycosides, and two hydroquinone derivatives (Fig. S1, Table 4). Below, we present only a brief description of the tentative structural identification of all these categories of specialized metabolites, as the variation of their profiles between extracts was evaluated from a multivariate analytical approach, what is described in the subsequent section.

3.2.1. Hydroxybenzoic/hydroxycinnamic and other organic acid derivatives

Four hydroxybenzoic acid derivatives were tentatively annotated, with two free acids [syringic acid (**4**, *m/z* 197.0456) and dihydroxybenzoic acid (**6**, *m/z* 153.0198), hydroxybenzoic acid (**7**, *m/z* 137.0248)] and one conjugate [vanillic acid hexoside (**11**, *m/z* 329.0878)]. Their assignment was performed on the basis of their HRMS, MS/MS data and comparison with fragmentation fingerprints described in the literature (González, Lanzelotti, & Luis, 2017; Taamalli et al., 2015). The free acids characteristically afforded decarboxylated (–CO_2, 44 Da) fragment ions, whereas the conjugate additionally provided the deglycosylated (-hexosyl, 162 Da) fragment ion. Moreover, five hydroxycinnamic acid derivatives were putatively assigned. Chlorogenic acid (**13**, *m/z* 353.0892), coumaroylquinic acid (**18**, *m/z* 337.0926), feruloylquinic acid (**20**, *m/z* 367.1035) showed the specific quinate ion at *m/z* 191.0516; in addition, the deprotonated, dehydrated and/or decarboxylated ions of the hydroxycinnamic acid residues were frequently observed. Rosmarinic acid (**29**, *m/z* 359.0766) afforded fragment ions at *m/z* 197.0437 [dihydroxyphenylactate]$^{-}$, 179.0353 [caffeate]$^{-}$, 161.0245 [anhydrocaffeate]$^{-}$ and 135.0470 [decarboxycaffeate]$^{-}$; these spectrometric data were consistent with the previous literature reports (Taamalli et al., 2015; Zengin et al., 2019). In comparison with this, peak **37** (*m/z* 373.0911, $C_{19}H_{18}O_8$) indicated the additional presence of a methylene group, suggesting the putative structure of methyl rosmarinate (Abedini et al., 2013). In addition, peaks **1**, **5**, and **10** were proposed as quinic acid, hydroxyphenylacetic acid, and benzoic acid (Taamalli et al., 2015). Previous LC-MS-based metabolite profiling of *Origanum* species has revealed a very similar profile of phenolic acids, with chlorogenic and rosmarinic acids being present among the most representative constituents in *O. majorana* (Taamalli et al., 2015), *O.* × *majoricum* Cambess. (González et al., 2017), *O. sipyleum* L. (Zengin et al., 2019), *O. boissieri* Ietsw., *O. saccatum* P.H. Davis, *O. solymicum* P.H. Davis or *O. hypericifolium* O.Schwarz & P.H. Davis (Özer et al., 2020).

Table 1
The AChE inhibitory activity of the extracts.

	O. majorana		*O. onites*		*O. syriacum*		*O. vulgare* subsp. *hirtum*		*O. vulgare*	
	Inhibition % ± S.E.M.[a]	IC_{50} (μg/ml)	Inhibition % ± S.E.M.[a]	IC_{50} (μg/ml)	Inhibition % ± S.E.M.[a]	IC_{50} (μg/ml)	Inhibition % ± S.E.M.[a]	IC_{50} (μg/ml)	Inhibition % ± S.E.M.[a]	IC_{50} (μg/ml)
January	69.44 ± 1.32***	95.66	23.06 ± 0.79***	>200	13.38 ± 3.03***	>200	9.32 ± 1.12	>200	–	>200
February	61.33 ± 0.75***	>200	27.18 ± 3.23***	>200	23.90 ± 1.47**	>200	12.75 ± 1.98	>200	9.65 ± 0.39*	>200
March	45.33 ± 0.88***	>200	28.59 ± 2.32***	>200	29.24 ± 1.59***	>200	38.26 ± 2.22***	>200	33.82 ± 1.49***	>200
April	65.76 ± 2.84***	111.10	9.40 ± 1.54	>200	67.74 ± 0.43***	95.32	34.20 ± 1.91***	>200	72.05 ± 2.48***	125.30
May	57.49 ± 1.38***	110.60	46.96 ± 2.25***	>200	57.99 ± 2.92***	161.6	57.71 ± 2.69***	166.00	49.94 ± 1.66***	>200
June	73.03 ± 2.65***	98.94	19.18 ± 3.18**	>200	50.63 ± 2.03***	184.70	46.20 ± 1.72***	>200	42.91 ± 1.40***	>200
July	60.23 ± 2.97***	140.30	39.98 ± 2.75***	>200	42.96 ± 0.10***	>200	55.51 ± 0.37***	155.40	50.29 ± 3.17***	188.60
August	68.18 ± 0.58***	62.08	46.19 ± 0.34***	>200	37.78 ± 1.94***	>200	71.63 ± 1.15***	133.30	35.52 ± 6.81***	>200
September	75.95 ± 1.41***	73.86	22.15 ± 2.83***	>200	48.39 ± 7.67***	>200	34.08 ± 3.84***	>200	18.65 ± 1.90*	>200
October	48.19 ± 2.74***	>200	36.39 ± 1.04***	>200	74.41 ± 1.05***	106.40	55.15 ± 3.52***	189.50	32.91 ± 1.23***	>200
November	48.39 ± 4.57**	>200	28.93 ± 0.95***	>200	67.60 ± 3.44***	140.20	22.28 ± 2.08**	>200	22.58 ± 2.94**	>200
December	30.97 ± 2.58***	>200	26.73 ± 1.44***	>200	38.58 ± 1.48***	>200	53.32 ± 4.98***	152.70	18.37 ± 0.52*	>200
Galanthamine	95.50 ± 1.31***	1.78	95.50 ± 1.31***	1.78	95.50 ± 1.31***	1.78	95.50 ± 1.31***	1.78	95.50 ± 1.31***	1.78

[a] Standard error mean (n = 3), 200 μg/mL concentration.

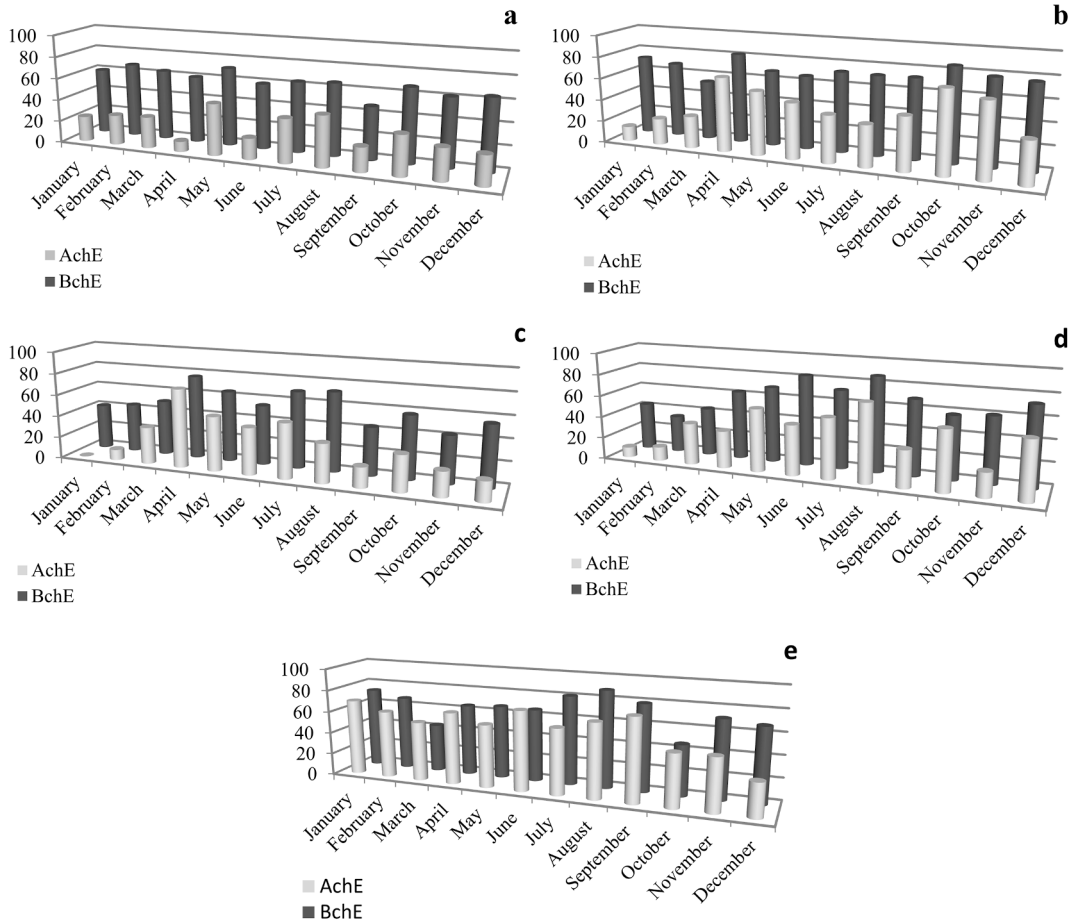


Fig. 1. The inhibitory activities of *Origanum onites* (a), *Origanum syriacum* (b), *Origanum vulgare* ssp. *viride* (c), *Origanum vulgare* ssp. *hirtum* (d), *Origanum majorana* (e) against AChE and BChE during the year.

3.2.2. Hydroquinone/cyclohexanone derivatives

Two hydroquinone derivatives were tentatively labeled, namely arbutin (**3**, *m/z* 271.0815) and caffeoylarbutin (**24**, *m/z* 433.1128), with their assignments performed by comparing their MS/MS fragment ions with those of compounds reported in *O. majorana*by Taamalli et al. (2015). Moreover, one cyclohexanone derivative, namely roseoside (**12**, *m/z* 385.1182), was tentatively identified. Its characteristic MS/MS fragments at *m/z* 223.1389 $[M-hexosyl-H]^-$, 179.0418 $[hexose-H]^-$, 161.0436 $[hexosyl-H]^-$ overlapped with those reported by Sun, Tao, and Zhang (2019).

3.2.3. Flavonoid derivatives

Flavonoids represented the most abundant constituents in the five species of *Origanum*, a number of 21 derivatives being spotted. Their assignments were majorly performed based on the characteristic fragment ions that appeared following *retro*-Diels-Alder (RDA) cleavages as thoughtfully detailed by Fabre, Rustan, Hoffmann, and Quetin-Leclercq (2001). The flavanol gallocatechin (**25**, *m/z* 305.0667) proved similar

Table 2
The BChE inhibitory activity of the extracts.

	O. majorana		*O. onites*		*O. syriacum*		*O. vulgare* subsp. *hirtum*		*O. vulgare*	
	Inhibition % ± S.E.M.[a]	IC_{50} (μg/ml)	Inhibition % ± S.E.M.[a]	IC_{50} (μg/ml)	Inhibition % ± S.E.M.[a]	IC_{50} (μg/ml)	Inhibition % ± S.E.M.[a]	IC_{50} (μg/ml)	Inhibition % ± S.E.M.[a]	IC_{50} (μg/ml)
January	73.36 ± 1.88***	62.03	60.39 ± 1.19***	119.40	72.55 ± 0.67***	87.85	43.69 ± 0.70***	>200	41.35 ± 4.06***	>200
February	67.73 ± 0.10***	88.87	67.81 ± 1.21***	99.00	68.68 ± 0.11***	131.20	34.04 ± 1.83***	>200	44.71 ± 0.31***	>200
March	43.84 ± 2.96***	>200	64.26 ± 1.49***	116.00	54.01 ± 1.23***	175.70	44.39 ± 0.43***	>200	50.69 ± 1.39***	180.10
April	65.21 ± 2.93***	102.60	60.94 ± 0.82***	134.60	82.11 ± 1.16***	69.49	63.41 ± 0.83***	90.67	76.80 ± 2.35***	77.35
May	67.03 ± 1.54***	66.68	71.68 ± 0.49***	78.94	68.75 ± 2.43***	104.4	69.94 ± 3.18***	61.01	65.11 ± 1.27***	100.10
June	66.44 ± 2.63***	65.49	59.79 ± 0.03***	163.10	66.81 ± 2.48***	93.60	83.34 ± 1.15***	56.71	54.75 ± 2.73***	152.50
July	81.46 ± 1.61***	50.56	64.29 ± 2.93***	115.90	73.03 ± 2.63***	84.05	72.41 ± 1.21***	58.36	70.27 ± 1.16***	77.64
August	88.97 ± 2.57***	29.00	65.99 ± 2.69***	85.84	72.37 ± 1.40***	64.75	87.28 ± 2.11***	45.86	72.62 ± 2.73***	70.05
September	79.55 ± 0.22***	64.53	48.04 ± 0.87***	>200	72.96 ± 1.66***	82.47	69.55 ± 1.76***	71.49	44.12 ± 1.66***	>200
October	46.46 ± 1.13***	>200	67.68 ± 0.89***	95.85	85.66 ± 3.68***	40.19	58.23 ± 3.17***	159.00	57.82 ± 1.15***	117.80
November	71.78 ± 0.00***	77.67	62.21 ± 1.18***	131.60	78.69 ± 2.15***	66.84	60.76 ± 1.20***	107.70	43.27 ± 1.90***	>200
December	68.23 ± 1.75***	95.91	64.87 ± 0.77***	85.08	77.14 ± 2.30***	58.19	73.27 ± 1.72***	118.00	55.95 ± 1.62***	142.20
Galanthamine	87.51 ± 0.24***	12.56	87.51 ± 0.24***	12.56	87.51 ± 0.24***	12.56	87.51 ± 0.24***	12.56	87.51 ± 0.24***	12.56

[a] Standard error mean (n = 3), 200 μg/mL concentration.

Table 3
The antioxidant activity of the extracts by metal-chelation activity and FRAP assays.

	Metal-chelation activity (Chelation% ± S.E.M.[a] at 2000 μg/ml[b])					FRAP[c] (Absorbance at 700 nm ± S.E.M.)				
	O. majorana	*O. onites*	*O. syriacum*	*O. vulgare* subsp. *hirtum*	*O. vulgare*	*O. majorana*	*O. onites*	*O. syriacum*	*O. vulgare* subsp. *hirtum*	*O. vulgare*
January	-[d]	2.23 ± 1.36	5.14 ± 1.18	14.11 ± 1.53***	11.32 ± 1.51	0.64 ± 0.016	0.99 ± 0.00	1.37 ± 0.04	0.26 ± 0.04	0.68 ± 0.04
February	–	4.77 ± 1.18	7.86 ± 6.73	3.04 ± 0.68	22.05 ± 3.20**	0.62 ± 0.035	0.94 ± 0.05	1.57 ± 0.06	1.09 ± 0.05	0.85 ± 0.02
March	–	8.45 ± 1.89	8.24 ± 1.36	2.90 ± 0.65	14.34 ± 6.92*	1.05 ± 0.064	0.80 ± 0.06	1.10 ± 0.03	0.68 ± 0.03	0.82 ± 0.02
April	–	33.04 ± 2.01***	6.75 ± 3.02	1.43 ± 0.32	11.71 ± 1.27	0.88 ± 0.033	0.88 ± 0.05	0.75 ± 0.05	0.68 ± 0.07	0.77 ± 0.02
May	–	2.01 ± 1.49	7.22 ± 0.70	7.43 ± 0.18*	10.87 ± 0.09	1.00 ± 0.018	0.90 ± 0.09	0.90 ± 0.06	0.88 ± 0.03	0.82 ± 0.03
June	15.68 ± 1.95***	5.82 ± 0.83	7.09 ± 0.09	–	–	0.76 ± 0.078	0.87 ± 0.08	0.78 ± 0.02	1.12 ± 0.06	0.64 ± 0.01
July	–	1.72 ± 2.42	5.81 ± 1.91	–	–	1.12 ± 0.049	0.58 ± 0.04	0.83 ± 0.01	1.03 ± 0.03	0.97 ± 0.02
August	5.12 ± 1.18	6.25 ± 2.01	13.63 ± 0.04*	–	–	0.97 ± 0.035	0.65 ± 0.07	0.68 ± 0.01	0.72 ± 0.03	0.42 ± 0.02
September	–	8.80 ± 0.66	4.24 ± 0.79	54.96 ± 1.52***	–	0.801 ± 0.021	0.85 ± 0.01	0.72 ± 0.05	0.62 ± 0.03	0.58 ± 0.01
October	5.93 ± 0.86	14.00 ± 0.83	8.27 ± 1.84	13.28 ± 1.82***	–	0.64 ± 0.041	0.81 ± 0.03	0.76 ± 0.05	0.68 ± 0.00	0.93 ± 0.04
November	–	9.85 ± 1.18	5.09 ± 4.86	5.17 ± 0.50	–	0.82 ± 0.023	0.76 ± 0.03	0.68 ± 0.06	0.99 ± 0.03	0.79 ± 0.08
December	5.05 ± 2.45	5.05 ± 0.00	5.88 ± 1.18	–	–	0.69 ± 0.012	0.95 ± 0.02	0.64 ± 0.07	0.96 ± 0.03	0.72 ± 0.01
Reference	97.19 ± 0.07[e]					1.79 ± 0.02[f]				

[a] Standard error mean (n = 3), [b] Stock solution for metal-chelation and FRAP assays, [c] Higher absorbance indicates greater antioxidant activity, [d] No activity, [e] EDTA tested at 2000 μg/ml.
[f] Quercetin tested at 1000 μg/ml.

HR-MS and MS/MS spectral data with those reported by Hossain, Rai, Brunton, Martin-Diana, and Barry-Ryan (2010). In the flavanone family, eriodictyol (**28**, *m/z* 287.0564) and naringenin (**39**, *m/z* 271.0601) gave fragment ions that overlapped with those observed by Zengin et al. (2019). For instance, the fragment ions at *m/z* 151.0067, 135.0491 and 107.0133 of eriodictyol were assigned as $^{1,3}A^-$, $^{1,3}B^-$ and $^{1,3}A^-$–CO_2 ions, respectively (Fabre Rustan, Hoffmann, & Quetin-Leclercq, 2001). A number of nine flavones were tentatively labeled as luteolin (**35**, *m/z* 285.0395), sorbifolin (**36**, *m/z* 299.0569), thymusin (**38**, *m/z* 329.0678), thymonin (**41**, *m/z* 359.0776) apigenin (**42**, *m/z* 269.0467), cirsimaritin (**50**, *m/z* 313.0716), pebrellin (**51**, *m/z* 343.0840), cirsilineol (**54**, *m/z* 343.0840) and genkwanin (**56**, *m/z* 283.0620). All these structures were previously reported in *Origanum* species (Skoula, Grayer, Kite, & Veitch, 2008; Taamalli et al., 2015; Zengin et al., 2019). For instance, the fragment ions at *m/z* 267.0395, 150.9991 and 133.0310 of luteolin were assigned as $[M-H_2O-H]^-$, $^{1,3}A^-$ and $^{1,3}B^-$ ions, respectively. In addition to the RDA fragmentation, the methoxylated flavones (cirsimaritin, cirsilienol, thymonin, etc) specifically afforded fragment ions obtained after losses CH_3 groups (15 Da), usually correlated with the degree of their methylation. Peak **43** (*m/z* 285.0397) was putatively annotated as kaempferol; its fragment ions at *m/z* 257.0479 $[M-CO-H]^-$, 229.0479 $[M-CO-H]^-$ and 151.0148 $[^{1,3}A]^-$ were in agreed with Fabre et al. (2001). Having a nominal mass with 2 Da higher, compound **33** (*m/z* 287.0560) was tentatively proposed as aromadendrin (dihydrokaempferol), whereas peak **27** (*m/z* 303.0889) as taxifolin (Taamalli et al., 2015). In addition to the above mentioned free aglycons, a number of six conjugated flavonoids were observed. For instance, peak **19** (*m/z* 593.1512) exhibited fragment ions at *m/z* 533.0686 $[M-CH_2O-H]^-$, 503.0895 $[M-C_2H_4O_2-H]^-$, 473.0857 $[M-C_4H_8O_3-H]^-$, 383.0592 $[M-C_4H_8O_3-C_3H_6O_3-H]^-$ and 353.0513 $[M-2\times C_4H_8O_3\text{-}H]^-$; these neutral losses [$CH_2O$ (30 Da), $C_2H_4O_2$ (60 Da), $C_3H_6O_3$ (90 Da) and $C_4H_8O_3$ (120 Da)] that appeared due to cross-

Table 4
LC-HRMS/MS metabolite profiling of *Origanum* spp.

No.	T_R [min]	UV abs λmax [nm]	$[M-H]^-_{exp}$ [*m/z*]	$[M-H]^-_{calcd}$ [*m/z*]	Δ [ppm]	MF	MS/MS (-) [*m/z*]	Identification	Chemical class	References
1	1.0	267	191.0566	191.0561	−2.54	$C_7H_{12}O_6$	173.0431; 127.0395	Quinic acid	Organic acid	Taamalli et al. (2015)
2	1.2	260; 285	290.0816	290.0823	2.29	$C_{18}H_{13}NO_3$	254.0779; 230.0625; 200.0560; 170.0438; 128.0348	Lysicamine	Oxoaporphine alkaloid	–
3	1.4	220; 280	271.0815	271.0823	3.04	$C_{12}H_{16}O_7$	108.0297	Arbutin	Hydroquinone glycoside	Taamalli et al. (2015)
4	3.1	255; 280	197.0456	197.0455	−0.27	$C_9H_9O_5$	179.0297; 135.0450; 123.0436	Syringic acid	Phenolic acid	Taamalli et al. (2015)
5	3.2	220; 280	151.0400	151.0401	0.45	$C_8H_8O_3$	123.0425; 105.0335	Hydroxyphenylacetic acid	Phenolic acid	–
6	4.0	260; 294	153.0198	153.0193	−3.04	$C_7H_6O_4$	109.0281	Dihydroxybenzoic acid	Phenolic acid	Taamalli et al. (2015)
7	5.3	nd	137.0248	137.0244	−2.77	$C_7H_6O_3$	109.0291	Hydroxybenzoic acid	Phenolic acid	–
8	6.1	250	349.1860	349.1868	2.26	$C_{16}H_{30}O_8$	187.1308; 161.0418	*p*-Menthane-1,2,3-triol hexoside I	Monoterpene glycoside	She et al., 2012
9	6.8	250	349.1876	349.1868	−2.31	$C_{16}H_{30}O_8$	187.1308; 161.0418	*p*-Menthane-1,2,3-triol hexoside II	Monoterpene glycoside	She et al., 2012
10	7.3	nd	121.0290	121.0295	4.12	$C_7H_6O_2$	109.9904	Benzoic acid	Organic acid	–
11	7.6	285	329.0887	329.0878	−2.71	$C_{14}H_{18}O_9$	167.0385; 123.0468	Vanillic acid hexoside	Phenolic acid glycoside	–
12	8.2	255; 285; 325	385.1882	385.1868	−3.65	$C_{19}H_{30}O_8$	223.1389; 205.1289; 161.0436; 153.0897	Roseoside	Cyclohexanone glycoside	Sun et al. (2019)
13	8.7	255; 290; 325	353.0892	353.0878	−3.94	$C_{16}H_{18}O_9$	191.0634; 179.0418; 173.0493; 135.0456	Chlorogenic acid	Phenolic acid	Taamalli et al. (2015)
14	9.0	255	387.1679	387.1661	−4.75	$C_{18}H_8O_9$	207.0956; 163.0432, 101.0243	Tuberonic acid hexoside	Fatty acid glycoside	Taamalli et al. (2015)
15	9.1	255	327.1456	327.1449	−2.05	$C_{16}H_{24}O_7$	165.0842	Thymoquinol hexoside	Monoterpene glycoside	Kamel et al. (2001)
16	9.5	255; 285	322.0942	322.0932	−3.02	$C_{15}H_{17}NO_7$	262.0827; 202.0571; 160.0447; 143.0382; 116.0481	Glucosylindole carboxylate	Alkaloid	–
17	9.8	255	225.1137	225.1132	−2.07	$C_{12}H_{18}O_4$	163.0487; 147.0827; 123.0425	Tuberonic acid	Fatty acid	Taamalli et al. (2015)
18	10.5	310	337.0926	337.0929	0.86	$C_{16}H_{18}O_8$	191.0516; 173.0461; 163.0430; 145.0271; 119.0451	Coumaroylquinic acid	Phenolic acid	–
19	10.9	270; 320	593.1531	593.1512	−3.21	$C_{27}H_{30}O_{15}$	533.0686; 503.0895; 473.0857; 383.0592; 353.0513	Apigenin-di-*C*-hexoside	Flavonoid glycoside	Taamalli et al. (2015)
20	11.3	254; 290; 320	367.1044	367.1035	−2.57	$C_{17}H_{20}O_9$	191.0514; 175.0423	Feruloylquinic acid	Phenolic acid	Zengin et al. (2019)
21	12.2	260	331.1753	331.1762	2.79	$C_{16}H_{28}O_7$	169.0834	*p*-Menth-1-ene-3,4-diol hexoside	Monoterpene glycoside	Kamel et al. (2001)
22	13.0	215; 260	391.1030	391.1035	1.16	$C_{19}H_{20}O_9$	281.0631; 137.0254; 109.0271	Unknown	–	–
23	13.1	250; 285; 335	463.0888	463.0882	−1.29	$C_{21}H_{20}O_{12}$	301.0355	Quercetin-*O*-hexoside	Flavonoid glycoside	Zengin et al. (2019)
24	13.7	265; 290	433.1128	433.1140	2.81	$C_{21}H_{22}O_{10}$	323.0738;161.0236; 133.0293; 109.0296	Caffeoylarbutin	Hydroquinone glycoside	Taamalli et al. (2015)
25	14.1	250; 285	305.0667	305.0667	−3.34	$C_{15}H_{14}O_7$	225.1131	Gallocatechin	Flavonoid	Taamalli et al. (2015)
26	14.6	254; 267; 340	447.0951	447.0933	−4.05	$C_{21}H_{20}O_{11}$	285.0334	Luteolin-*O*-hexoside	Flavonoid glycoside	Zengin et al. (2019)
27	15.3	260; 330	303.0889	303.0874	−4.89	$C_{16}H_{16}O_6$	285.0324; 206.9552; 175.3800	Taxifolin	Flavonoid	Taamalli et al. (2015)
28	16.1	290; 330	287.0564	287.0561	−1.00	$C_{15}H_{12}O_6$	151.0067; 135.0491, 107.0133	Eriodictyol	Flavonoid	Taamalli et al. (2015)
29	16.9	220; 245; 290; 330	359.0766	359.0772	1.78	$C_{18}H_{16}O_8$	197.0437; 179.0353; 161.0245; 135.0470	Rosmarinic acid	Phenolic acid	Taamalli et al. (2015)
30	18.0	285; 330	593.1514	593.1512	−0.35	$C_{27}H_{30}O_{15}$	447.0893; 285.0322	Luteolin-*O*-rhamnosylhexoside	Flavonoid glycoside	Zengin et al. (2019)
31	18.5		519.1298	519.1297	−0.25	$C_{28}H_{24}O_{10}$	259.0597; 153.0184; 109.0271	Unknown	–	–

(*continued on next page*)

Table 4 (*continued*)

No.	T_R [min]	UV abs λmax [nm]	$[M-H]^-_{exp}$ [*m*/*z*]	$[M-H]^-_{calcd}$ [*m*/*z*]	Δ [ppm]	MF	MS/MS (-) [*m*/*z*]	Identification	Chemical class	References
		260; 290; 325								
32	18.7	260; 290; 340	591.1355	591.1355	0.07	$C_{27}H_{28}O_{15}$	531.1123; 285.0381	Luteolin-*O*-acetyldipentoside	Flavonoid glycoside	Zengin et al. (2019)
33	18.9	285; 330	287.0560	287.0561	0.39	$C_{15}H_{12}O_6$	151.0671; 127.0332	Aromadendrin	Flavonoid	–
34	20.3	260; 290; 340	623.1235	623.1254	3.00	$C_{27}H_{28}O_{17}$	447.0639; 323.0764; 299.0507; 285.0218;	Luteolin-*O*-glucuronylhexoside	Flavonoid glycoside	–
35	20.5	250; 285; 340	285.0395	285.0405	3.36	$C_{15}H_{10}O_6$	267.0395; 150.9991; 133.0310	Luteolin	Flavonoid	Taamalli et al. (2015)
36	20.6	285; 340	299.0569	299.0561	−2.63	$C_{16}H_{12}O_6$	284.0337; 271.0216; 151.0031	Sorbifolin	Flavonoid	Skoula et al. (2008)
37	20.7	290; 330	373.0911	373.0929	4.79	$C_{19}H_{18}O_8$	193.0584; 179.0347; 161.0173; 135.0479	Methylrosmarinate	Phenolic acid	Abedini et al. (2013)
38	20.9	245; 285; 345	329.0678	329.0667	−3.40	$C_{17}H_{14}O_7$	314.0434; 299.0179; 271.0268	Thymusin	Flavonoid	Skoula et al. (2008)
39	21.8	225; 280	271.0601	271.0612	4.03	$C_{15}H_{12}O_5$	227.0700; 177.0210; 151.0048; 119.0506	Naringenin	Flavonoid	Zengin et al. (2019)
40	21.9	290; 330	327.2176	327.2177	0.30	$C_{18}H_{32}O_5$	314.0418; 299.0191; 271.0296; 229.1441; 171.1070	Trihydroxyoctadecadienoic acid I	Fatty acid	Taamalli et al. (2015)
41	22.4	255; 285; 340	359.0776	359.0772	−1.00	$C_{18}H_{16}O_8$	344.0545; 329.0324; 314.0291; 301.0414	Thymonin	Flavonoid	Skoula et al. (2008)
42	23.1	260; 335	269.0467	269.0455	−4.27	$C_{15}H_{10}O_5$	151.0671; 127.0332	Apigenin	Flavonoid	Taamalli et al. (2015)
43	23.4	265; 365	285.0397	285.0405	2.66	$C_{15}H_{10}O_6$	257.0479; 229.0479; 151.0148	Kaempferol	Flavonoid	Fabre et al. (2001)
44	23.5	255; 330	329.2335	329.2333	−0.76	$C_{18}H_{34}O_5$	314.0397; 229.1444; 211.1341; 171.1078	Trihydroxyoctadecenoic acid	Fatty acid	Nastić, Borrás-Linares, Lozano-Sánchez, Švarc-Gajić, and Segura-Carretero (2020)
45	23.7	260	165.0924	165.0921	−1.79	$C_{10}H_{14}O_2$	150.0702	Unknown	–	–
46	24.1	290; 330	327.2192	327.2177	−4.58	$C_{18}H_{32}O_5$	314.0418; 299.0191; 271.0296; 229.1441; 171.1070	Trihydroxyoctadecadienoic acid II	Fatty acid	Taamalli et al. (2015)
47	24.5	290; 340	345.1719	345.1707	−3.33	$C_{20}H_{26}O_5$	330.1366; 315.1609; 301.1794; 283.1413	Rosmanol	Diterpene	Hossain et al. (2010)
48	24.8	255	287.2235	287.2228	−2.49	$C_{16}H_{32}O_4$	228.0620	Dihydroxyhexadecanoic acid	Fatty acid	–
49	24.9	240; 290	347.1876	347.1864	−3.45	$C_{20}H_{28}O_5$	273.1380; 231.0943; 217.0766	Unknown	–	–
50	26.1	275; 290	313.0716	313.0718	0.51	$C_{17}H_{14}O_6$	298.0471; 283.0219; 255.0312	Cirsimaritin	Flavonoid	Hossain et al. (2010)
51	26.4	270; 330	343.0840	343.0823	−4.86	$C_{18}H_{16}O_7$	328.0550; 313.0305; 298.0114; 270.0162	Pebrellin	Flavonoid	Skoula et al. (2008)
52	27.0	320	361.1658	361.1657	−0.38	$C_{20}H_{26}O_6$	346.1428; 316.1266; 287.1204; 273.1113	Hydroxyrosmanol	Diterpene	–
53	27.3	250; 315	307.1923	307.1915	−2.65	$C_{18}H_{28}O_4$	289.1803; 235.1339; 211.1334; 185.1181; 121.0644	Unknown	–	–
54	27.8	276	343.0823	343.0823	0.08	$C_{18}H_{16}O_7$	328.0550; 313.0305; 298.0114; 270.0162	Cirsilineol	Flavonoid	Skoula et al. (2008)
55	28.7	240; 290	347.1876	347.1864	−3.45	$C_{20}H_{28}O_5$	329.1746; 231.1025; 217.0870	Unknown	–	–
56	29.2	265; 280; 330	283.0620	283.0612	−2.83	$C_{16}H_{12}O_5$	268.0393; 239.0362; 211.0410; 151.0033; 117.0343	Genkwanin	Flavonoid	Skoula et al. (2008)
57	29.8	280; 330	311.2237	311.2228	−2.94	$C_{18}H_{32}O_4$	293.2085; 253.1793; 223.1693; 161.0077	Hydroperoxyoctadecadienoic acid	Fatty acid	Taamalli et al. (2015)
58	30.4	280; 330	329.1763	329.1758	−1.41	$C_{22}H_{26}O_4$	285.1734; 186.0698; 127.0761	Carnosol I	Diterpene	Hossain et al. (2010)
59	30.9	280; 330	331.1935	331.1915	−4.87	$C_{20}H_{28}O_4$	290.1063; 259.1300; 236.8110; 201.0826	Carnosic acid	Diterpene	Hossain et al. (2010)

(*continued on next page*)

Table 4 (*continued*)

No.	T_R [min]	UV abs λmax [nm]	$[M-H]^-_{exp}$ [*m/z*]	$[M-H]^-_{calcd}$ [*m/z*]	Δ [ppm]	MF	MS/MS (-) [*m/z*]	Identification	Chemical class	References
60	31.8	280; 330	311.1651	311.1653	0.54	$C_{20}H_{24}O_3$	268.1054; 224.0825; 175.0748; 163.0774; 135.0824	Unknown	–	–
61	32.3	275; 330	435.1448	435.1449	0.29	$C_{25}H_{24}O_7$	407.1513; 323.2069; 287.0596; 259.0627; 189.0855; 125.0264	Unknown	–	–
62	32.8	280; 330	329.1759	329.1758	0.20	$C_{22}H_{26}O_4$	285.1734; 186.0698; 127.0761	Carnosol II	Diterpene	Hossain et al. (2010)
63	33.5	nd	419.1559	419.1559	−0.04	$C_{18}H_{28}O_{11}$	299.0844; 271.0448; 227.0561; 177.0074; 150.9917	Unknown	–	–
64	33.8	255	433.1292	432.1293	0.18	$C_{25}H_{22}O_7$	418.1029; 299.0560; 256.0560; 203.0686; 119.0482	Unknown	–	–
65	34.1	260	583.2346	583.2396	−3.06	$C_{28}H_{40}O_{13}$	433.1380; 287.0607; 259.0576	Unknown	–	–
66	35.2	235	293.2125	293.2122	−0.96	$C_{18}H_{30}O_3$	275.2050; 183.1374; 171.1023; 121.1023	Hydroxyoctadecatrienoic acid I	Fatty acid	Nastić et al. (2020)
67	35.4	235	293.2133	293.2122	−3.68	$C_{18}H_{30}O_3$	275.2050; 183.1374; 171.1023; 121.1023	Hydroxyoctadecatrienoic acid II	Fatty acid	Nastić et al. (2020)
68	35.7	235	293.2120	293.2122	0.74	$C_{18}H_{30}O_3$	275.2050; 183.1374; 171.1023; 121.1023	Hydroxyoctadecatrienoic acid III	Fatty acid	Nastić et al. (2020)
69	36.8	nd	419.1544	419.1559	3.54	$C_{18}H_{28}O_{11}$	299.0844; 271.0448; 227.0561; 177.0074; 150.9917	Unknown	–	–
70	37.2	nd	243.1964	243.1966	0.69	$C_{14}H_{28}O_3$	221.1529; 193.0953	Unknown	–	–
71	37.5	230	295.2270	295.2279	2.93	$C_{18}H_{32}O_3$	277.2158; 181.1225; 171.1008	Hydroxyoctadecadienoic acid I	Fatty acid	Nastić et al. (2020)
72	37.9	230	295.2269	295.2279	3.27	$C_{18}H_{32}O_3$	277.2158; 181.1225; 171.1008	Hydroxyoctadecadienoic acid II	Fatty acid	Nastić et al. (2020)
73	38.1	230	295.2265	295.2279	4.62	$C_{18}H_{32}O_3$	277.2158; 181.1225; 171.1008	Hydroxyoctadecadienoic acid III	Fatty acid	Nastić et al. (2020)

ring cleavage of the hexose units were supporting a *C*-glycosylation, indicating the structure of apigenin-di-*C*-hexoside, a compound previously reported in *O. majorana* (Taamalli et al., 2015) as well as in *O. spyleum* (Zengin et al., 2019). On the other hand, the isobaric peak **30** (*m/z* 593.1512) led to assigning its structure as luteolin-*O*-rhamnosylhexoside; this was indicated by its fragment ions at *m/z* 447.0893 $[M-rhamnosyl-H]^-$ and 285.0322 $[M-rhamnosyl-glucosyl-H]^-$. Furthermore, the MS/MS spectra of peaks **26** (*m/z* 447.0951), **32** (*m/z* 591.1355) and **34** (*m/z* 623.1235) suggested the same aglycon as the previous compound, their structures being thus proposed as *O*-hexoside, *O*-acetyldipentoside, and *O*-glucuronylhexoside of luteolin, respectively. The nature of their sugar units was indicated by specific neutral losses, such as 162 Da (hexosyl), 132 Da (pentosyl) or 176 Da (glucuronyl). Lastly, the main fragment ion at *m/z* 301.0355 of peak **23** (*m/z* 463.0888) hinted the presence of quercetin as the aglycon; this compound was tentatively labeled as quercetin-*O*-hexoside (Zengin et al., 2019).

3.2.4. Terpene derivatives

Four compounds were annotated as monoterpene derivatives. Two isobaric monoterpene conjugates (**8** and **9**) gave $[M-H]^-$ at *m/z* 349.1868; their MS/MS spectra diagnostically exhibited fragment ions at *m/z* 187.1308 $[M-hexosyl-H]^-$ and 161.0418 $[hexosyl-H]^-$. These data were in agreement with She, Xu, and Liu (2012) for *p*-menthane-1,2,3-triol hexoside, previously isolated from *Mentha haplocalyx* Briq. Similar fragmentation patterns were observed in the structures tentatively proposed as thymoquinol hexoside (**15**, *m/z* 327.1459) and *p*-menth-1-ene-3,4-diol hexoside (**21**, *m/z* 331.1753); these two compounds were formerly reported in *O. syriacum* (Kamel et al., 2001). In addition, a series of five compounds were putatively identified as abietane diterpene derivatives. Rosmanol (**47**, *m/z* 345.1719) showed particular fragment ions at *m/z* 301.1794 $[M-CO_2-H]^-$ and 283.1413 $[M-CO_2-H_2O-H]^-$. Having one additional oxygenated function, compound **52** (*m/z* 361.1657) was tentatively assigned as hydroxyrosmanol. Furthermore, the two isobaric compounds at *m/z* 329.1758 (**58** and **62**) behaved in a similar manner with rosmanol, being putatively labeled as carnosol isomers, whereas peak **59** (*m/z* 331.1935) was annotated as carnosic acid. Except the suggested structure of hydroxyrosmanol, the other abietane diterpenes were previously reported by Hossain et al. (2010) in *O. majorana*.

3.2.5. Fatty acids derivatives

Two jasmonate derivatives, namely tuberonic acid (**17**, *m/z* 225.1137) and its conjugate tuberonic acid hexoside (**14**, *m/z* 387.1679), were recognized based on their most suggestive fragment ion at *m/z* 163.0887 $[tuberonate-CO_2-H_2O]^-$; these compounds were also annotated in *O. majorana* by Taamalli et al. (2015). Additionally, 11 acyclic oxygenated fatty acids were tentatively labeled, with $[M-H]^-$ at *m/z* 327.2176 (**40** and **46**), 329.2335 (**44**), 287.2235 (**48**), 311.2237 (**57**), 293.2125 (**66**–**68**) and 295.2270 (**71**–**73**). This kind of fatty acids were previously reported in *Origanum* species (Taamalli et al., 2015), their significant number in the current extracts being potentially related to the polarity of the extraction solvent (ethanol) that can considerably solubilize non-polar constituents.

3.3. Correlation analysis

The correlation coefficients between the tentatively identified compounds (absolute peak areas of each assigned peak from the base peak chromatograms) and the bioactivity results (IC_{50} values of all bioassays) were calculated for all 60 extracts of *Origanum* species (Table 5). The non-significant correlations are given in italics, whereas normal font was used for 95% confidence and bold for 99% confidence levels.

Significant correlations were observed between aromadendrin (**33**) and AChE, BChE, and FRAP results. The inhibitory activity of aromadendrin against AChE (IC_{50} = 173.22 μM) and BChE (IC_{50} = 95.13 μM)

Table 5
Correlation coefficients between the tentatively annotated metabolites (absolute peak areas) and bioactivity results (IC_{50} values). Statistical significance is marked by font: boldface means 99% significance, normal font 95% significance, italic font lack of significance at 95%.

No.	Specialized metabolite	AChE	BChE	Metal-chelation	FRAP	DPPH radical scavenging
1	Quinic acid	*0.187*	*0.166*	**0.338**	*−0.007*	*−0.147*
2	Lysicamine	0.272	*−0.04*	*−0.213*	*0.002*	*0.104*
3	Arbutin	*0.109*	*−0.077*	*−0.153*	*−0.042*	*0.137*
4	Syringic acid	*0.014*	*−0.100*	**0.507**	*−0.060*	*−0.019*
5	Hydroxyphenylacetic acid	*−0.104*	*−0.039*	*0.033*	**0.408**	*0.211*
6	Dihydroxybenzoic acid	0.261	*0.127*	*−0.066*	*0.047*	*−0.096*
7	Hydroxybenzoic acid	*0.225*	*0.111*	*−0.069*	0.287	0.271
8	*p*-Menthane-1,2,3-triol hexoside I	*−0.319*	*−0.222*	**0.519**	*−0.072*	*−0.083*
9	*p*-Menthane-1,2,3-triol hexoside II	*−0.309*	*−0.313*	**0.478**	*−0.247*	*0.091*
10	Benzoic acid	*−0.126*	*−0.007*	**0.448**	*−0.226*	*−0.208*
11	Vanillic acid hexoside	*0.187*	*0.153*	*−0.071*	*0.038*	*−0.143*
12	Roseoside	**0.406**	*0.094*	*−0.225*	*0.161*	*0.048*
13	Chlorogenic acid	*0.030*	0.298	*0.031*	*0.244*	*0.203*
14	Tuberonic acid hexoside	**0.363**	*0.029*	*−0.187*	*0.094*	*0.029*
15	Thymoquinol hexoside	*0.103*	*0.101*	*−0.108*	*0.131*	*−0.044*
16	Glucosylindole carboxylate	*−0.269*	*−0.076*	*−0.056*	*−0.105*	*−0.034*
17	Tuberonic acid	**0.308**	*0.187*	*−0.090*	*0.165*	*−0.030*
18	Coumaroylquinic acid	*0.094*	*−0.208*	*0.152*	*−0.011*	*0.210*
19	Apigenin-di-*C*-hexoside	*0.167*	*−0.015*	*−0.033*	*0.135*	*0.010*
20	Feruloylquinic acid	*0.183*	**0.360**	*−0.112*	*0.041*	*−0.012*
21	*p*-Menth-1-ene-3,4-diol hexoside	**0.480**	*0.180*	*−0.167*	*0.213*	*−0.044*
23	Quercetin-*O*-hexoside	*0.091*	*0.049*	*−0.140*	*−0.192*	*−0.028*
24	Caffeoylarbutin	**0.507**	**0.345**	*−0.110*	*0.137*	*−0.167*
25	Gallocatechin	*−0.073*	*−0.17*	*−0.041*	*−0.038*	*0.084*
26	Luteolin-*O*-hexoside	*0.204*	*−0.043*	*0.053*	*−0.127*	*0.034*
27	Taxifolin	*0.12*	*0.078*	*−0.181*	0.297	**0.384**
28	Eriodictyol	**0.565**	**0.323**	*−0.145*	*0.057*	*−0.174*
29	Rosmarinic acid	*0.223*	*0.050*	*−0.189*	0.287	**0.386**
30	Luteolin-*O*-rhamnosylhexoside	**0.468**	0.280	*−0.222*	*0.160*	*−0.017*
32	Luteolin-*O*-acetyldipentoside	*−0.391*	*−0.127*	*−0.015*	*0.104*	*0.215*
33	Aromadendrin	**0.514**	**0.445**	*−0.202*	**0.367**	*0.011*
34	Luteolin-*O*-glucuronylhexoside	*0.116*	*−0.033*	*−0.008*	*0.086*	*0.007*
35/36	Luteolin/Sorbifolin*	0.291	*0.22*	*0.136*	*0.037*	*−0.248*
37/38	Methyl rosmarinate/Thymusin*	0.286	**0.337**	*−0.089*	*0.135*	*−0.059*
39	Naringenin	*0.120*	*0.091*	*0.003*	*−0.037*	*−0.139*
40	Trihydroxyoctadecadienoic acid I	**0.490**	0.266	*−0.093*	*0.177*	*−0.029*
41	Thymonin	0.269	**0.305**	*−0.079*	*−0.054*	*−0.085*
42	Apigenin	**0.497**	0.255	*−0.062*	*0.135*	*−0.078*
43	Kaempferol	*0.086*	*0.134*	*0.059*	*−0.169*	*−0.156*
44	Trihydroxyoctadecenoic acid	*0.026*	*0.174*	*−0.177*	*0.067*	*0.117*
46	Trihydroxyoctadecadienoic acid II	*−0.377*	*−0.166*	0.282	*0.153*	*0.193*
47	Rosmanol	*−0.095*	*0.059*	0.251	*−0.089*	*−0.192*
48	Dihydroxyhexadecanoic acid	**0.462**	*0.226*	*−0.129*	*0.115*	*0.008*
50	Cirsimaritin	**0.31**	0.272	*0.24*	*0.042*	*−0.210*
51	Pebrellin	**0.381**	0.250	*−0.013*	*0.066*	*−0.145*
52	Hydroxyrosmanol	*−0.275*	*−0.204*	*−0.079*	*−0.108*	*−0.048*
54	Cirsilineol	*−0.142*	*0.020*	*−0.155*	*−0.146*	*−0.107*
56	Genkwanin	**0.384**	0.289	*−0.105*	*0.129*	*−0.206*
57	Hydroperoxyoctadecadienoic acid	*−0.150*	*−0.271*	*0.005*	*0.065*	*0.143*
58	Carnosol I	*0.069*	*0.145*	*0.183*	*−0.253*	*0.127*
59	Carnosic acid	*0.162*	*0.201*	*−0.212*	*0.083*	*0.061*
62	Carnosol II	0.265	*0.236*	*−0.292*	*−0.078*	*−0.006*
66	Hydroxyoctadecatrienoic acid I	*0.224*	*−0.010*	*−0.144*	*0.100*	*−0.064*
67	Hydroxyoctadecatrienoic acid II	*−0.118*	*−0.207*	*−0.086*	*0.035*	*0.156*
68	Hydroxyoctadecatrienoic acid III	*−0.050*	*−0.214*	*0.193*	*−0.052*	*0.201*
71	Hydroxyoctadecadienoic acid I	*0.208*	*0.211*	*−0.103*	*−0.068*	*−0.025*
72	Hydroxyoctadecadienoic acid II	*−0.159*	*−0.090*	*−0.035*	*−0.091*	*−0.044*
73	Hydroxyoctadecadienoic acid III	*−0.372*	*−0.368*	0.269	*0.133*	**0.352**

*These compounds co-eluted, so their peak areas were extracted together.

was shown in a previous study conducted by Muhammad et al. (2015). Aromadendrin also exerted antioxidant activity *via* lipid peroxidation (IC_{50} = 45.62 μM) and ABTS cation radical scavenging (IC_{50} = 153.51 μM) activities (Muhammad et al., 2015). Caffeoyl arbutin (**24**) and eriodictyol (**28**) were also found to correlate with the AChE and BChE inhibitory activities of the extracts. Many studies demonstrated the anti-Alzheimer effect of eriodictyol acting *via* different mechanisms. A bioactivity-guided study for the determination of active molecules of the *Drynariae* rhizome against AChE led to the isolation of eriodictyol as the main compound responsible for this activity. Eriodictyol inhibited AChE with IC_{50} value of 7.19 μM (Liu et al., 2020). Besides that, the activity of eriodictyol on the lipopolysaccharide (LPS)-induced amyloidogenesis, neuroinflammation and cognitive impairment was revealed in a study conducted on C57BL/6J mice. The results of the study demonstrated that eriodictyol (100 mg/kg) decreased the AChE activity (0.1996 U/mgprot), increased the ACh level (5.093 μg/mgprot) and ChAT activity (41.81 U/g), while diminishing the formation of $A\beta_{1-42}$. Additionally, eriodictyol inhibited NF-κB and MAPK pathways; therefore, it regulated cytokines and inflammatory mediators (He et al., 2018). In a study, the inhibitory activity of eriodictyol on advanced glycation end products (AGEs), which are associated with AD, eriodictyol inhibited the formation of AGEs (Liu et al., 2020). At the same time, eriodictyol could cross

the blood–brain barrier (BBB) (Mani et al., 2015). The crossing of BBB is important for the therapeutic approach of neurodegenerative disorders, such as AD (Roney et al., 2005). In addition, pebrellin (**51**), genkwanin (**56**), apigenin (**42**), cirsimaritin (**50**), dihydroxyhexadecanoic acid (**46**), luteolin-*O*-rhamnosylhexoside (**30**), *p*-menth-1-ene-3,4-diol hexoside (**21**), roseoside (**12**), trihydroxyoctadecadienoic acid I (**40**), tuberonic acid (**17**), and tuberonic acid hexoside (**14**) were also found to be correlated in various extents with the AChE inhibitory effect of the extracts (Table 5).

The specialized metabolites formed in plants and their amounts can vary with environmental, genetic, physiological and agricultural factors (Ahmed et al., 2019). In a study conducted on the essential oil and extract of *O. onites* leaves, the influence of the harvest time from June to September on the phenolic compounds, essential oil composition and antioxidant activities were studied. While the extraction yield was found highest in September, total phenolic content, free-radical scavenging and reducing/antioxidant activities as well as the levels of vitexin, rutin, naringin, hesperidin and rosmarinic acid displayed the highest values in July. On the other hand, the acacetin content of the extract was highest in June (Ozkan, Baydar, & Erbas, 2010).

In a study by Christensen and Grevsen (2006), the influence of the region, harvest time and region on the chemical composition of *O. ehrenbergii* essential oils was evaluated. For this purpose, the essential oils were distilled from plants harvested for two years in two regions and dried using shade-drying at 4 °C and lyophilization. It was found that the yield of the essential oils was higher from June to July, whereas the amount of the major compound, carvacrol, was higher from March to October. On the other hand, thymoquinone content was observed higher in January and February. It was shown that the different drying techniques, soil characteristics, geographical factors and location did not affect the yield and composition of the essential oils of *O. ehrenbergii* (Zgheib et al., 2019). In another study conducted on the essential oils of *Origanum vulgare* ssp. *hirtum* by Christensen and Grevsen (2006), the content of carvacrol was higher in July than in October, whilst the content of *p*-cymene was higher in October than in July.

3.4. Simulated binding energies for aromadendrin, caffeoylarbutin, and eriodictyol

In order to estimate the free binding energies of the systems upon forming their complexes, the interactions of atoms between the ligands and their targets (AChE and BChE) were simulated using docking simulation methods. Galanthamine, used as a reference compound in the simulation, showed the highest binding energies in the both complexes. This can demonstrate that all the three selected compounds have a significant improvement towards binding to the active site domains. Ligand binding energies of aromadendrin, caffeoylarbutin, eriodictyol and galanthamine were calculated and presented using box plot including the first, second and third quartiles, along with the outliers of the data (Fig S2). Caffeoylarbutin revealed the lowest binding energy in both targets, with median values lower than −10 kcal/mol. Both aromadendrin- and eriodictyol-bound AChE had the lowest binding energies in comparison to those for BChE complexes.

4. Conclusions

Due to the wide spectrum of biological activities, the species belonging to *Origanum* genus are very popular herbal medicinal plants used for the production of various food supplements. However, both the quality and biological activity may depend on species, chemotype, geographic origin, and time of collection throughout the year. In our experiments, the bioactivity and phytochemical evaluation of different *Origanum* species collected throughout a 12-month period cultivated around the Mediterranean region of Turkey was performed. The possible links between the phytochemical fingerprints of the extracts and their corresponding activities were scrutinized *via* phytochemical correlation analysis, which provides an alternative method for screening for potential bioactive compounds. Several specialized metabolites, such as aromadendrin, were pointed out as possessing meaningful correlations with AChE, BChE, and FRAP activities. This study provides a basis for agricultural or pharmaceutical applications of the studied *Origanum* species and constitutes an alternative method to screen for the potential active compounds without conventional and time-consuming phytochemical separation and purification processes; thus, the association of phytochemical correlation analysis with bioassay results can be an excellent strategy for pointing out the bioactive metabolites from complex plant crude extracts as implemented in the current study.

CRediT authorship contribution statement

Hasya Nazli Gök: Investigation, Methodology. **Simon Vlad Luca:** Methodology, Validation, Formal analysis, Investigation, Data curation, Writing – original draft. **Saadet Tugrul Ay:** Investigation, Methodology. **Łukasz Komsta:** Conceptualization, Formal analysis, Software. **Ramin Ekhteiari Salmas:** Investigation, Methodology. **Ilkay Erdogan Orhan:** Conceptualization, Funding acquisition, Project administration, Supervision, Writing - review & editing. **Krystyna Skalicka-Woźniak:** Conceptualization, Funding acquisition, Project administration, Supervision, Writing - review & editing.

Declaration of Competing Interest

The authors declare that they have no known competing financial interests or personal relationships that could have appeared to influence the work reported in this paper.

Acknowledgements

This work was supported with the funds provided by Medical University of Lublin DS28.

Appendix A. Supplementary data

Supplementary data to this article can be found online at https://doi.org/10.1016/j.foodchem.2021.130775.

References

Abedini, A., Roumy, V., Mahieux, S., Biabiany, M., Standaert-Vitse, A., Rivière, C., … Hennebelle, T. (2013). Rosmarinic acid and its methyl ester as antimicrobial components of the hydromethanolic extract of *Hyptis atrorubens* Poit. (Lamiaceae). *Evidence-Based Complementary and Alternative Medicine, 2013*, 1–11. https://doi.org/10.1155/2013/604536.

Ahmed, S., Griffin, T. S., Kraner, D., Schaffner, M. K., Sharma, D., Hazel, M., … Cash, S. B. (2019). Environmental factors variably impact tea secondary metabolites in the context of climate change. *Frontiers in Plant Science, 10*. https://doi.org/10.3389/fpls.2019.00939.

Brookmeyer, R., Johnson, E., Ziegler-Graham, K., & Arrighi, H. M. (2007). Forecasting the global burden of Alzheimer's disease. *Alzheimer's & Dementia, 3*(3), 186–191. https://doi.org/10.1016/j.jalz.2007.04.381.

Budimir, A. (2011). Metal ions, Alzheimer's disease and chelation therapy. *Acta Pharmaceutica, 61*, 1–14. https://doi.org/10.2478/v10007-011-0006-6.

Cheung, et al. (2012). Structures of human acetylcholinesterase in complex with pharmacologically important ligands. *Journal of Medicinal Chemistry*. https://doi.org/10.1021/jm300871x.

Christensen, L. P., & Grevsen, K. (2006). Effect of development stage at harvest on the composition and yield of essential oils from thyme and oregano. In W. Bredie, & M. Petersen (Eds.), *Developments in Food Science* (vol. 43, pp. 261–264). Elsevier.

Chua, M.-T., Tung, Y.-T., & Chang, S.-T. (2008). Antioxidant activities of ethanolic extracts from the twigs of *Cinnamomum osmophloeum*. *Bioresource Technology, 99*(6), 1918–1925. https://doi.org/10.1016/j.biortech.2007.03.020.

Darvesh, S., Cash, M. K., Reid, G. A., Martin, E., Mitnitski, A., & Geula, C. (2012). Butyrylcholinesterase is associated with β-amyloid plaques in the transgenic APPSWE/PSEN1dE9 mouse model of Alzheimer Disease. *Journal of Neuropathology and Experimental Neurology, 71*(1), 2–14. https://doi.org/10.1097/NEN.0b013e31823cc7a6.

Ellman, G. L., Courtney, K. D., Andres, V., & Featherstone, R. M. (1961). A new and rapid colorimetric determination of acetylcholinesterase activity. *Biochemical Pharmacology, 7*(2), 88–95.

Fabre, N., Rustan, I., Hoffmann, E., & Quetin-Leclercq, J. (2001). Determination of flavone, flavonol, and flavanone aglycones by negative ion liquid chromatography electrospray ion trap mass spectrometry. *Journal of Ameican Society of Mass Spectrometry, 12*(6), 707–715. https://doi.org/10.1016/S1044-0305(01)00226-4.

Farid, R., Day, T., Friesner, R. A., & Pearlstein, R. A. (2006). New insights about HERG blockade obtained from protein modeling, potential energy mapping, and docking studies. *Bioorganic and Medicinal Chemistry, 14*(9), 3160–3173. https://doi.org/10.1016/j.bmc.2005.12.032.

González, M. D., Lanzelotti, P. L., & Luis, C. M. (2017). Characterization of the polyphenolic fingerprint of *Origanum* × *majoricu*m Cambess. from Argentina by high-performance liquid chromatography and multivariate analysis. *Food Analytical Methods, 10*(10), 3275–3284. https://doi.org/10.1007/s12161-017-0894-2.

Hatano, Tsutomu, Kagawa, Harumi, Yasuhara, Taeko, & Okuda, Takuo (1988). Two new flavonoids and other constituents in licorice root: Their relative astringency and radical scavenging effects. *Chemical and Pharmaceutical Bulletin, 36*(6), 2090–2097.

He, P., Yan, S., Zheng, J., Gao, Y., Zhang, S., Liu, Z., … Xiao, C. (2018). Eriodictyol attenuates LPS-induced neuroinflammation, amyloidogenesis, and cognitive impairments *via* the inhibition of NF-κB in male C57BL/6J mice and BV2 microglial cells. *Journal of Agricultural and Food Chemistry, 66*(39), 10205–10214. https://doi.org/10.1021/acs.jafc.8b03731.

Honda, G., Yeşilada, E., Tabata, M., Sezik, E., Fujita, T., Takeda, Y., … Tanaka, T. (1996). Traditional medicine in Turkey VI. Folk medicine in West Anatolia: Afyon, Kütahya, Denizli, Muğla, Aydin provinces. *Journal of Ethnopharmacology, 53*(2), 75–87. https://doi.org/10.1016/S0378-8741(96)01426-2.

Hossain, M. B., Rai, D. K., Brunton, N. P., Martin-Diana, A. B., & Barry-Ryan, C. (2010). Characterization of phenolic composition in Lamiaceae spices by LC-ESI-MS/MS. *Journal of Agriculture and Food Chemistry, 58*(19), 10576–10581. https://doi.org/10.1021/jf102042g.

Kamel, M. S., Assaf, M. H., Hasanean, H. A., Ohtani, K., Kasai, R., & Yamasaki, K. (2001). Monoterpene glucosides from *Origanum syriacum*. *Phytochemistry, 58*(8), 1149–1152. https://doi.org/10.1016/S0031-9422(01)00386-7.

Kosak, et al. (2016). Development of an in-vivo active reversible butyrylcholinesterase inhibitor. *Scientific Reports*. https://doi.org/10.1038/srep39495.

Liu, J., Yang, Z., Cheng, Y.e., Wu, Q., He, Y., Li, Q., & Cao, X. (2020). Eriodictyol and naringenin inhibit the formation of AGEs: An *in vitro* and molecular interaction study. *Journal of Molecular Recognition, 33*(1). https://doi.org/10.1002/jmr.v33.110.1002/jmr.2814.

Liu, M.-Y., Zeng, F., Shen, Y., Wang, Y.-Y., Zhang, N., & Geng, F. (2020). Bioguided isolation and structure identification of acetylcholinesterase enzyme inhibitors from *Drynariae* rhizome. *Journal of Analytical Methods in Chemistry, 2020*, 1–9. https://doi.org/10.1155/2020/2971841.

Luca, S. V., Czerwinska, M. E., Miron, A., Aprotosoaie, A. C., Marcourt, L., Wolfender, J. L., … Skalicka-Wozniak, K. (2019). High-performance countercurrent chromatographic isolation of acylated iridoid diglycosides from *Verbascum ovalifolium* Donn ex Sims and evaluation of their inhibitory potential on IL-8 and TNF-alpha production. *Journal of Pharmaceutical and Biomedical Analysis, 166*, 295–303. https://doi.org/10.1016/j.jpba.2019.01.031.

Madhavi Sastry, G., Adzhigirey, M., Day, T., Annabhimoju, R., & Sherman, W. (2013). Protein and ligand preparation: Parameters, protocols, and influence on virtual screening enrichments. *Journal of Computer-Aided Molecular Design, 27*(3), 221–234. https://doi.org/10.1007/s10822-013-9644-8.

Mani, R. J., Mittal, K., Mishra, S., Kharkwal, H., Ahmad, S., & Katare, D. P. (2015). In silico approach to evaluate the efficacy of dietary flavonoids and their role in Alzheimer's disease. *International Journal of Pharmaceutical Sciences Review and Research, 34*, 94–102.

Marrelli, M., Statti, G. A., & Conforti, F. (2018). *Origanum* spp.: An update of their chemical and biological profiles. *Phytochemistry Reviews, 17*(4), 873–888. https://doi.org/10.1007/s11101-018-9566-0.

Moreira, P. I., Santos, M. S., Oliveira, C. R., Shenk, J. C., Nunomura, A., Smith, M. A., … Perry, G. (2008). Alzheimer disease and the role of free radicals in the pathogenesis of the disease. *CNS Neurological Disorders and Drug Targets, 7*, 3–10. https://doi.org/10.2174/187152708783885156.

Muhammad, A., Tel-Cayan, G., Öztürk, M., Nadeem, S., Duru, M. E., Anis, I., … Shah, M. R. (2015). Biologically active flavonoids from *Dodonaea viscosa* and their structure–activity relationships. *Industrial Crops and Products, 78*, 66–72. https://doi.org/10.1016/j.indcrop.2015.10.011.

Naquvi, K. J., Ahamad, J., Salma, A., Ansari, S. H., & Najmi, A. K. (2019). A critical review on traditional uses, phytochemistry and pharmacological uses of *Origanum vulgare* Linn. *International Research Journal of Pharmacy, 10*(3), 7–11. https://doi.org/10.7897/2230-840710.7897/2230-8407.100310.7897/2230-8407.100370.

Nastić, N., Borrás-Linares, I., Lozano-Sánchez, J., Švarc-Gajić, J., & Segura-Carretero, A. (2020). Comparative assessment of phytochemical profiles of comfrey (*Symphytum officinale* L.) root extracts obtained by different extraction techniques. *Molecules, 25*(4), 837. https://doi.org/10.3390/molecules25040837.

Oyaizu, M. (1986). Studies on products of browning reaction. *Japanese Journal of Nutrition and Dietetics, 44*, 307–315. https://doi.org/10.5264/eiyogakuzashi.44.307.

Özer, Z., Gören, A. C., Kılıç, T., Öncü, M., Çarıkçı, S., & Dirmenci, T. (2020). The phenolic contents, antioxidant and anticholinesterase activity of section *Amaracus* (Gled.) Vogel and *Anatolicon* Ietsw. of *Origanum* L. species. *Arabian Journal of Chemistry, 13*(4), 5027–5039. https://doi.org/10.1016/j.arabjc.2020.01.025.

Ozkan, G., Baydar, H., & Erbas, S. (2010). The influence of harvest time on essential oil composition, phenolic constituents and antioxidant properties of Turkish oregano (*Origanum onites* L.). *Journal of Science of Food and Agriculture, 90*(2), 205–209. https://doi.org/10.1002/jsfa.3788.

Roney, C., Kulkarni, P., Arora, V., Antich, P., Bonte, F., Wu, A., … Aminabhavi, T. M. (2005). Targeted nanoparticles for drug delivery through the blood-brain barrier for Alzheimer's disease. *Journal of Controlled Release, 108*(2-3), 193–214. https://doi.org/10.1016/j.jconrel.2005.07.024.

She, G.-M., Xu, C., & Liu, B. (2012). New monocyclic monoterpenoid glycoside from *Mentha haplocalyx* Briq. *Chemistry Central Journal, 6*(1). https://doi.org/10.1186/1752-153X-6-37.

Skoula, M., Grayer, R. J., Kite, G. C., & Veitch, N. C. (2008). Exudate flavones and flavanones in *Origanum* species and their interspecific variation. *Biochemical Systematics and Ecology, 36*(8), 646–654. https://doi.org/10.1016/j.bse.2008.05.003.

Sun, L., Tao, S., & Zhang, S. (2019). Characterization and quantification of polyphenols and triterpenoids in thinned young fruits of ten pear varieties by UPLC-Q TRAP-MS/MS. *Molecules, 24*(1), 159. https://doi.org/10.3390/molecules24010159.

Taamalli, A., Arráez-Román, D., Abaza, L., Iswaldi, I., Fernández-Gutiérrez, A., Zarrouk, M., & Segura-Carretero, A. (2015). LC-MS-based metabolite profiling of methanolic extracts from the medicinal and aromatic species *Mentha pulegium* and *Origanum majorana*. *Phytochemical Analysis, 26*(5), 320–330. https://doi.org/10.1002/pca.v26.510.1002/pca.2566.

Weller, J., & Budson, A. (2018). Current understanding of Alzheimer's disease diagnosis and treatment. F1000Research, 7. https://doi.org/10.12688/f1000research.14506.1.

Yeşilada, E., Honda, G., Sezik, E., Tabata, M., Fujita, T., Tanaka, T., … Takaishi, Y. (1995). Traditional medicine in Turkey. V. Folk medicine in the inner Taurus Mountains. *Journal of Ethnopharmacology, 46*(3), 133–152.

Zengin, G., Ferrante, C., Orlando, G., Zheleva-Dimitrova, D., Gevrenova, R., Recinella, L., … Menghini, L. (2019). Chemical profiling and pharmaco-toxicological activity of *Origanum sipyleum* extracts: Exploring for novel sources for potential therapeutic agents. *Journal of Food Biochemistry, 43*(11). https://doi.org/10.1111/jfbc.v43.1110.1111/jfbc.13003.

Zgheib, R., El-Beyrouthy, M., Chaillou, S., Ouaini, N., Rutledge, D., Stien, D., … Iriti, M. (2019). Chemical variability of the essential oil of *Origanum ehrenbergii* Boiss. from Lebanon, assessed by independent component analysis (ICA) and common component and specific weight analysis (CCSWA). *International Journal of Molecular. Science, 20*(5), 1026. https://doi.org/10.3390/ijms20051026.